2011 IEEE International Conference on Rehabilitation Robotics
Rehab Week Zurich, ETH Zurich Science City, Switzerland, June 29 - July 1, 2011

On the Development of a Walking Rehabilitation Device with a Large Workspace

Clément Gosselin and Thierry Laliberté

Abstract— **Rehabilitation therapy aiming at helping a person to regain or improve the ability to walk is a labour-intensive activity. In this context, the patient is often limited to very restricted walking spaces. This paper presents a device that can support the weight of a person walking freely over a large workspace. The device is based on an overhead gantry mechanism combined with a cable routing that decouples the vertical motion from the horizontal displacements of the person. The mechanical architecture is first presented and it is shown that the principle can be applied to the design of a completely passive device in which the portion of the weight to be supported can be adjusted. A simplified dynamic model is also derived in order to highlight the characteristics of the device. A powered version of the device is then discussed. Finally, a prototype of a passive device built at full scale is presented and discussed. A video accompanying the paper illustrates the experimental tests underway with the prototype.**

I. Introduction

Bipedal walking is a mechanically complex activity that involves the coordination of many muscles based on a variety of sensing inputs. Therefore, the rehabilitation of patients with walking disabilities requires learning, which can in turn translate into long hours of exercises. Moreover, assisting a person that requires support to walk is a difficult task. If the person is assisted only by therapists, then several of them are needed which becomes very costly. On the other hand, if the person is supported by a harness, the walking space is usually very limited (e.g. a treadmill is used) which is a significant drawback, especially in advanced stages of the learning process.

The development of devices to assist in the rehabilitation of patients with walking disabilities has been addressed by several research groups. Two main issues have been considered, namely the support of the patient and the guidance of his/her limbs. Most of the proposed concepts are based on a the use of a treadmill (see [1] and [2] for instance). Although treadmills offer some advantages in terms of footprint and control, they cannot reproduce the real dynamics of walking because the inertia of the upper body of the patient is not included in the walking scenario. Other similar devices have also been developed for applications in the support of elderly people (see for instance [3]).

In [4], a robotic assistive device is used to support the weight of the patient. The portion of the weight to be supported can be adjusted. However, the workspace available to the patient is limited and the floor footprint of the device is rather large.

Mobile robotic devices that 'follow' the patient have also been developed (see for instance [5] and [6]) in order to increase the workspace and allow the patient to walk naturally on a floor. However, this approach involves a large mobile robot that requires significant floor space and raises issues regarding the safe active control of the robot.

In other approaches, robotic platforms are attached to the feet of the user and controlled directly (see for instance [7], [8] and [9]). Such systems are similar to the use of treadmills regarding the walking simulation, although they provide more flexibility and allow the simulation of obstacles, stairs and others. In [10], a walking rehabilitation device based on a cable-driven parallel mechanism is proposed. This concept leads to an effective light-weight apparatus and allows the application of controlled forces to the person. However, it also requires the use of a treadmill with the patient walking on the spot. In [11], a robotic system suspended from a ceiling-mounted rail is proposed. This device allows the patient to walk more naturally on a floor. However, deviations from a linear path and changes of direction are not possible. Other commercial systems based on some of the concepts mentioned above are also available (see for instance [12] and [13]).

This paper presents a new device that aims at providing a large walking space while supporting the weight of the patient. The proposed concept allows the user to walk freely on a floor in all directions, including changes of rotation, over a large workspace. The device naturally leads itself to a passive mechanism but can also be implemented as an active robotic system. After presenting the basic principle of the device, its implementation as a passive mechanism or as an active robotic system is discussed. A dynamic model is then studied to highlight the design challenges. Finally, the experimental validation on a full-scale prototype is presented and some conclusions are drawn.

II. Mechanical architecture

A. Four-degree-of-freedom gantry mechanism

The device proposed in this work is based on an overhead gantry mechanism similar to those commonly found in industrial settings. Two parallel rails attached to the ceiling provide the motion travel in one horizontal direction. A bridge is suspended to these rails. A trolley is suspended to the bridge on a rail orthogonal to the first set of rails. The trolley provides the motion travel in the second horizontal direction. A vertical slider mechanism is attached to the trolley and provides the third degree of freedom, i.e., vertical

This work was supported by The Natural Sciences and Engineering Research Council of Canada (NSERC) as well as the Canada Research Chair program.

The authors are with the Department of Mechanical Engineering, Université Laval, Québec, Québec, Canada, G1V 0A6, gosselin@gmc.ulaval.ca, thierry@gmc.ulaval.ca

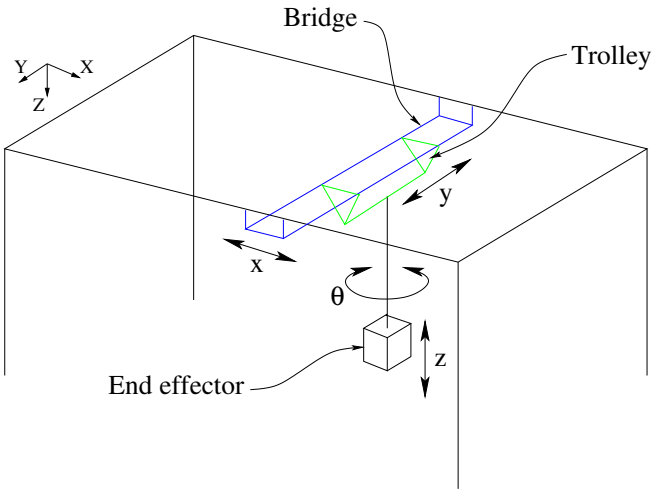

Fig. 1. Schematic representation of the 4-dof gantry structure.

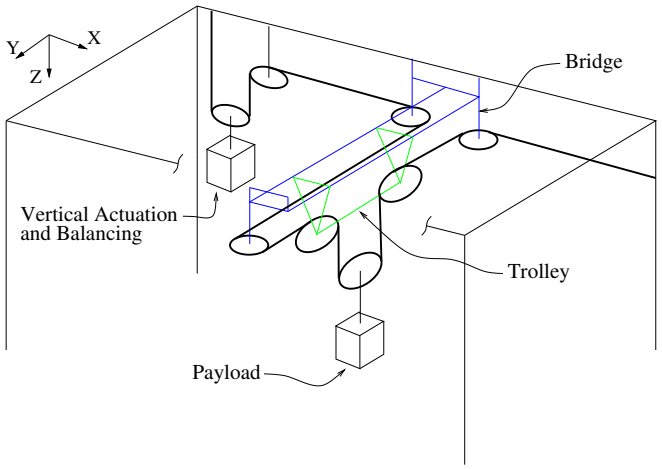

Fig. 2. Cable routing for the weight compensation mechanism.

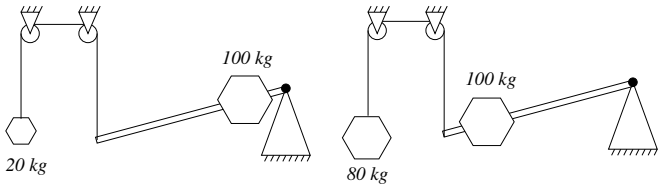

Fig. 3. Adjustable weight compensation mechanism.

translation. Finally, a revolute joint with a vertical axis can be added in order to allow the end body to rotate freely around a vertical axis. Alternatively, the vertical slider and the rotation can be replaced by a cable hoist. The four degrees of freedom of the mechanism correspond to the so-called Schönflies motions or SCARA motions. The kinematic architecture of the gantry mechanism is illustrated schematically in Fig. 1. One advantage of an overhead gantry mechanism is that it does not occupy any of the floor space.

B. Weight compensation

The overhead gantry mechanism described in the preceding subsection provides the degrees of freedom required to allow a person to walk freely in all directions, including a rotation around a vertical axis. However, the vertical degree of freedom must provide a force to balance the weight (or part of the weight) of the person. In other words, the main objective of this mechanism is to be able to *follow* the person with an overhead support and compensate part of its weight. One effective means of supporting the weight of the person is to use an adjustable counterweight mounted on the vertical slider mechanism. However, mounting the counterweight directly on the vertical slider would significantly increase the inertia of the moving bodies of the mechanism, thereby leading to a large inertia in the horizontal directions. In a passive system, this inertia would be highly detrimental because it would require the person to *drag* a significant additional mass. Therefore, it is desired to move the counterweight away from the person and mount it on the fixed frame.

A cable transmission using the routing illustrated in Fig. 2 can be used to move the counterweight to a fixed location. This arrangement basically connects the counterweight to the person via a cable transmission that cancels out the horizontal motions. Additionally, it is noted that the total length of cable in the routing is constant and therefore no spool is required. The motion of the counterweight is completely decoupled from the horizontal motions which means that horizontal motions of the mechanism leave the counterweight at rest. A motion of the counterweight is induced only when a vertical motion of the end-effector takes place. Therefore, the counterweight does not contribute to the horizontal inertia.

The weight compensation mechanism must be adjustable in order to accommodate variations on the weight of the user. Moreover, for a given user, the portion of the weight to be compensated may vary depending on the person's condition. It may also be desirable to change this parameter during a working session in order to test different walking conditions or vary the stimuli. Therefore, the counterweight is mounted on a rotating lever. Sliding the counterweight along the lever and locking it in different positions provides a simple and effective means of adjusting the weight compensation. The adjustable compensation mechanism is illustrated in Fig. 3.

It is clear from the above that the proposed device is well-suited for a passive assistive walking mechanism. Indeed, horizontal motions are provided by the bridge and trolley gantry mechanism which can be designed to induce limited friction and does not require large forces to be activated. Also, because of the cable transmission, the counterweight is mounted on a fixed pivoting lever and does not contribute to increasing the inertia in the horizontal directions. Finally, the adjustment of the mass to be compensated is easily performed by moving the counterweight along the lever arm.

III. Dynamic Modelling

A dynamic model is derived in order to determine the forces required to accelerate the mechanism when performing walking exercises. One can write

$$\mathbf{f} = \mathbf{f}_r + \mathbf{A}(\mathbf{p})\ddot{\mathbf{p}} + \mathbf{b}(\mathbf{p}, \dot{\mathbf{p}}) + \mathbf{c}(\mathbf{p}) \tag{1}$$

where $\mathbf{f}$ is the external force vector defined as

$$\mathbf{f} = [f_x \; f_y \; f_z \; \tau]^T, \tag{2}$$

$\mathbf{f}_r$ is the friction force vector defined as

$$\mathbf{f}_r = [f_{rx}\ f_{ry}\ f_{rz}\ \tau_r]^T, \tag{3}$$

$\mathbf{p}$ is the Cartesian position vector defined as

$$\mathbf{p} = [x\ y\ z\ \theta]^T, \tag{4}$$

in which x, y, z and θ are the position components in all directions, where θ is the rotation around the vertical axis, $\dot{\mathbf{p}}$ is the Cartesian velocity vector and $\ddot{\mathbf{p}}$ is the Cartesian acceleration vector defined as

$$\dot{\mathbf{p}} = \left[\dot{x}\ \dot{y}\ \dot{z}\ \dot{\theta}\right]^T, \quad \ddot{\mathbf{p}} = \left[\ddot{x}\ \ddot{y}\ \ddot{z}\ \ddot{\theta}\right]^T. \tag{5}$$

Matrix $\mathbf{A}$ describes the inertia of the system which can be written as

$$\mathbf{A} = \begin{bmatrix} M_{11} & 0 & 0 & 0 \\ 0 & M_{22} & 0 & 0 \\ 0 & 0 & M_{33} & 0 \\ 0 & 0 & 0 & I_z \end{bmatrix} \tag{6}$$

with

$$M_{11} = m_1 + m_2 + m_3 + m_h \tag{7}$$

$$M_{22} = m_2 + m_3 + m_h \tag{8}$$

and where m_1, m_2, m_3 and m_h are respectively the mass of the bridge, the mass of the trolley, the mass of the end-effector and the mass of the human subject while I_z is the inertia of the end-effector plus the human subject around the vertical axis. Vector $\mathbf{b}$ represents the so-called centrifugal and Coriolis terms

$$\mathbf{b} = [0\ 0\ B_3\ 0]^T, \tag{9}$$

whose components are all zero except for the vertical motion for which there is a nonlinear relationship between the motion of the end-effector and the counterweight. Vector $\mathbf{c}$ represents the terms arising from the potential energy of the system and can be written as

$$\mathbf{c} = [0\ 0\ C_3\ 0]^T, \tag{10}$$

whose components are all zero except for the vertical motion, which involves gravitational potential energy. The expressions for M_{33}, B_3 and C_3 will be given after the kinematics of the balancing system is established.

The geometry of the balancing system is described in Fig. 4. It can be seen that

$$z = \rho_o - \rho \tag{11}$$

with

$$\rho_o = \sqrt{h^2 + (l_o - l)^2}. \tag{12}$$

From the relationships

$$\rho \sin\phi = l_o - l\cos\psi \tag{13}$$

$$h - \rho\cos\phi = l\sin\psi \tag{14}$$

and eliminating ϕ, one can obtain ρ as

$$\rho = \sqrt{h^2 + {l_o}^2 + l^2 - 2l(h\sin\psi + l_o\cos\psi)}. \tag{15}$$

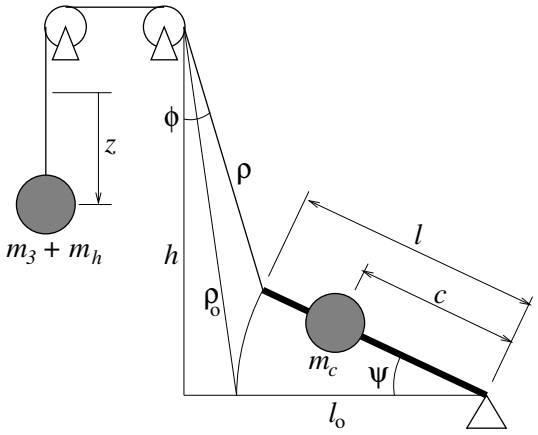

Fig. 4. Geometry of the balancing system.

The time derivative of eq. (11) gives

$$\dot{z} = \frac{l(h\cos\psi - l_o\sin\psi)\dot{\psi}}{\rho}. \tag{16}$$

In order to simplify the dynamic modelling and provide more insight, the following approximations are introduced. The lengths l_o and l are assumed to be approximately equal, h is assumed to be significantly larger than l_o and l, and ψ is kept relatively small, say less than 30 degrees. As a result, angle ϕ is small and $\cos\phi \simeq 1$. Then, eq.(11) is approximated by

$$z = l\sin\psi \tag{17}$$

and eq.(16) is approximated by

$$\dot{z} = \dot{\psi} l\cos\psi \tag{18}$$

The dynamic model is obtained using the Lagrangian approach

$$\frac{d}{dt}\left(\frac{\partial(T-V)}{\partial\dot{z}}\right) - \frac{\partial(T-V)}{\partial z} = f_z - f_{rz} \tag{19}$$

The kinetic energy T is

$$T = \frac{1}{2}(m_3 + m_h)\dot{z}^2 + \frac{1}{2}I_c\dot{\psi}^2 \tag{20}$$

where I_c is the inertia of the counterweight around its pivot. The potential energy V is

$$V = m_c g c\sin\psi - (m_3 + m_h)gz = (\frac{m_c c}{l} - m_3 - m_h)gz \tag{21}$$

where m_c is the mass of the counterweight. The result can then be included in eq. (1) which gives

$$M_{33} = m_3 + m_h + \frac{I_c}{l^2\cos^2\psi} \tag{22}$$

$$B_3 = \frac{\dot{z}^2 I_c\tan\psi}{l^3\cos^3\psi} \tag{23}$$

$$C_3 = \left(\frac{m_c c}{l} - m_3 - m_h\right)g. \tag{24}$$

In the mechanical architecture described in the preceding section, the trolley is mounted on the bridge and the vertical

slider is mounted on the trolley. Therefore one has, by inspection of eqs.(7) and (8),

$$M_{11} > M_{22} \tag{25}$$

Hence, considering eqs.(6) and (25), it is clear that the inertia is not equal in the two horizontal directions. This is a drawback of the bridge and trolley arrangement. In a passive system, it means that the spurious inertia felt by the user will not be the same depending on the direction of walking. Therefore, it is important that the design of the mechanism aims at minimizing m_1. Clearly, all masses should be minimized but the latter has the most impact on the performance of a passive device. Simulations can be performed based on the simplified dynamic model presented above in order to estimate the performances in terms of the horizontal forces required for walking. However, at low velocities, friction may be dominant and should therefore be estimated in a practical design.

Approximating the counterweight as a point mass, its inertia around the fixed pivot, noted I_c in the above equations, can be written as

$$I_c = m_c c^2. \tag{26}$$

The balancing ratio, noted γ, is defined as the ratio of the static moment of the counterweight with respect to the fixed pivot over the static moment generated by the payload on the pivot. In other words, when γ is equal to 1, the payload is exactly balanced. From eq.(24), one obtains

$$\gamma = \frac{m_c c}{(m_3 + m_h) l}. \tag{27}$$

The inertia ratio, noted α, is defined as the ratio of the effective inertia of the counterweight over the inertia of the payload. A small value of α is desirable in order to minimize the spurious inertia. From eqs.(22) and (26), one obtains

$$\alpha = \frac{m_c c^2}{l^2 \cos^2 \psi (m_3 + m_h)} = \frac{c\gamma}{l \cos^2 \psi}. \tag{28}$$

It can be observed that by using a larger counterweight mounted closer to the pivot, the total inertia associated with the vertical motion is reduced. This is so because the mass of the counterweight required to obtain static balancing increases linearly with the lever arm while the inertia increases quadratically. Therefore, in practice a large counterweight mounted close to the pivot is preferable and will lead to smaller spurious inertia (smaller values of α). It can also be observed that it is preferable to keep the lever around the horizontal configuration in order to avoid excessive inertia. This is obtained if the lever is sufficiently long compared to the total vertical displacement. Also, from eq.(23), it can be seen that the effect of I_c is limited if ψ and $\dot{z}$ are kept small.

IV. Powered assistive device

Although the device described above leads naturally to a passive mechanism, it is also possible to introduce actuation in order to improve the performances and reduce the spurious forces to be provided by the user due to the inertia and friction in the mechanism. To this end, actuators could be included directly on the joints of the gantry mechanism. However, this approach would further increase the inertia of the moving components. In order to circumvent this problem, closed-loop belt-driven transmissions are used. Several closed-loop transmissions were proposed in [14] for application in four-dof gantry mechanisms. The transmissions used here are based on the arrangements proposed in the latter reference. First, it is observed that because of the mechanical architecture of the grantry device, the inertia induced by the mechanism around the vertical axis of rotation is rather negligeable. Therefore, this degree of freedom is left passive and no actuation is required. Then, it is pointed out that the cable routing used to attach the payload to the counterweight can be used to locate the actuator providing the vertical motion on the base. Indeed, the actuator for the vertical motion can be mounted directly at the counterweight. Finally, the horizontal motions (bridge and trolley) are considered. Actuation is most relevant for these degrees of freedom since they are more likely to produce undesirable effects on the user.

The actuation of the bridge is based on the closed-loop transmission illustrated in Fig. 5-left. In this figure, the bridge is represented by a rectangle and the pulleys by circles. The $\times$s mark the places where the belt is attached to the bridge and the square around one of the circles denotes that the corresponding pulley is actuated. As it can be observed on the figure, the length of the closed loop is constant and therefore no spool is needed. Also, the forces applied on the bridge are well balanced and provide stability.

The actuation of the trolley is based on the closed-loop transmission illustrated in Fig. 5-right. Similarly to the preceding routing, the closed loop for the actuation of the trolley also has a constant length and does not require a spool. Moreover, it is pointed out that the two transmissions are completely decoupled. In other words, a motion of one of the actuators does not have any impact on the other degree of freedom and vice-versa. One important advantage of decoupling is that no antagonistic forces are generated, which makes the control easier and which reduces the power required at the actuators.

Using the above actuation schemes, it is possible to actuate the horizontal motions of the gantry mechanism and compensate for the inertia and friction in these directions by tracking the motion of the torso of the person.

V. Experimental validation

A passive 3-dof version of the concept described above was implemented experimentally for demonstration purposes. The mechanism built in the laboratory — shown in Fig. 6 — is based on a device that was developed for other applications (payload manipulation). The main modification is the addition of a chair as an interface between the human subject and the end-effector. Therefore, although it provides a proof of concept, the experimental set-up is not tailored to the application described here. First, the mechanism has only three degrees of freedom and does not allow rotations around the vertical axis, which is definitely a limitation

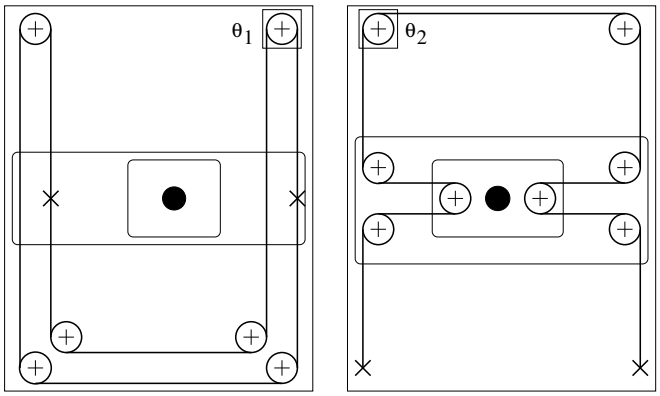

Fig. 5. Closed-loop belt-driven transmissions. Left: for the actuation of the bridge motion. Right: for the actuation of the trolley motion.

for walking devices. Additionally, the inertia of the bridge, trolley and end-effector could be significantly reduced since the prototype mechanism was developed for larger payloads.

Despite the aforementioned limitations, the experimental implementation performs rather well, as shown in the accompanying video. In particular, it can be observed that the gravity compensation is effective and well decoupled from horizontal motions. It is observed that for large balancing ratios ($\gamma > 0.8$), the static forces between the human subject and the floor are so small that it is difficult to perform horizontal accelerations by walking. The user tends to jump when trying to apply more force on the floor. It is also observed that for small balancing ratios ($\gamma < 0.2$) the prototype could not always follow the user, i.e., the chair separates from the subject when large upwards accelerations are performed. In order to avoid this phenomenon, the unloaded device (without the person) should be able to perform large upward accelerations. In other words, with $m_h = 0$, C_3 should be as large as possible compared to M_{33}. The use of a chair allowed to adapt a system intended for another application. However, the walking motion was not fully natural and comfort was limited. It is clear that a better interface, such as a harness, should be used in the future. Horizontal motions are also well demonstrated, although it is clear that friction and inertia should be reduced in a real implementation of the concept. As mentioned above, such a reduction should be possible in a design based on realistic requirements.

In order to verify the dynamic model along the vertical motion, position mesasurements were performed. Numerical differentiation of the position was then performed in order to obtain the velocity and acceleration. The results obtained can then be compared with the acceleration computed from eq.(1). The parameters of the prototype are as follows: $l = 1.0m$, $l_o = 0.96m$, $h = 2.2m$, $m_3 = 12kg$ and $m_h = 70kg$. For reasons related to other applications of the prototype, the range of motion of the lever is $-15^o < \psi < 30^o$. As a result, a person in a standing position with their feet on the floor corresponds to $z = 0.31m$ or $\psi = 18^o$. Also, the value of ϕ is comprised between -1^o and 1^o for 80% of the range of motion, with a maximum of 3^o. Therefore, the geometric

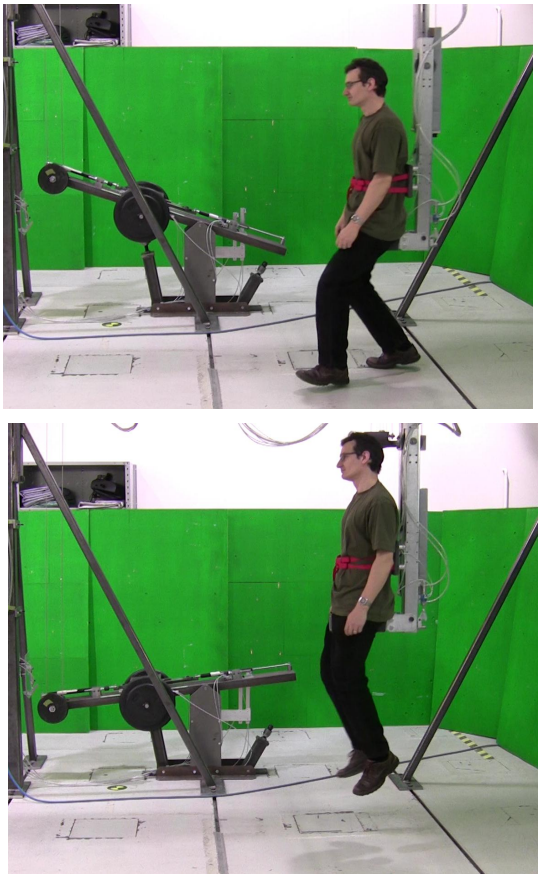

Fig. 6. Passive 3-dof assistive walking device built in the laboratory.

approximation used for the relation between z and ψ is applicable. From measurements taken with a dynamometer, the friction is estimated to be approximately $f_{rz} = 20N$.

Six balancing cases are studied. They are presented in Table I. Typical experimental curves are plotted in Fig. 7. Since the forces applied by the person on the floor are not known, the model can be verified only during the free-falling trajectory of the person jumping in the air. For the last two cases given in the table, since the balancing ratio is small, it is possible to manually 'throw' the chair downwards and measure the acceleration of the unloaded device. However, it is difficult for the person to stay in the air long enough to obtain effective measurements with the setup used.

TABLE I

THE SIX BALANCING CASES. THE ACCELERATIONS $\ddot{z}$ ARE CALCULATED AROUND THE POINT WHERE THE VELOCITY IS ZERO. THE CORRESPONDING MEASURED VALUES ARE GIVEN IN PARENTHESES.

Case	m_c (kg)	c (m)	γ	α $(\psi = 0)$	$\ddot{z}$ with person (m/s^2)	$\ddot{z}$ chair only (m/s^2)
C1	58	1.0	0.71	0.71	1.7 (1.8)	-5.6
C2	112	0.52	0.71	0.37	2.1 (2.0)	-9.4
C3	35	1.0	0.43	0.43	3.9 (4.0)	-4.2
C4	67	0.52	0.43	0.22	4.6 (4.4)	-6.6
C5	21	1.0	0.26	0.26	5.8	-2.3 (-2.2)
C6	33	0.64	0.26	0.16	6.3	-3.2 (-3.0)

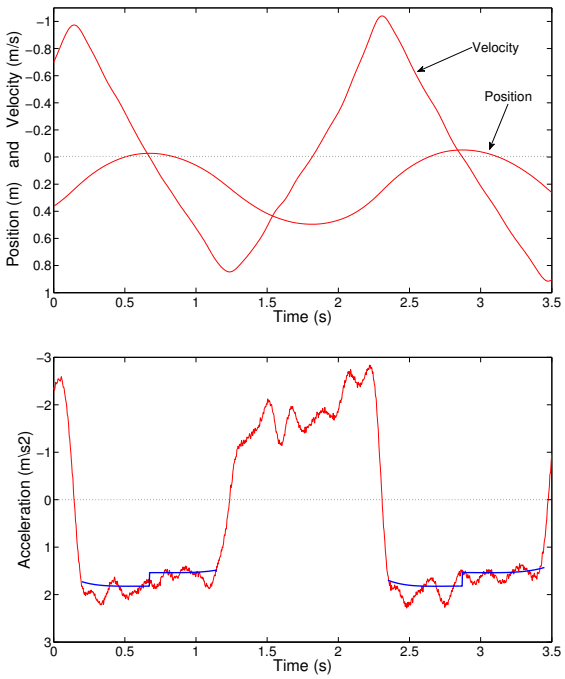

Fig. 7. Example of measured position, velocity and acceleration along z. Acceleration curves obtained from eq.1 are plotted during free-falling. The steps in the curves correspond to the change of direction of the friction force. The slight changes at the ends of the curves are due to the variation of ψ.

From the six cases studied, the effect of the balancing ratio (γ) on the acceleration is very clear. Also, the effect of the inertia ratio (α) is significant, especially on the unloaded device. Therefore, it is of interest to minimize the inertia in order to obtain better performances during the upwards acceleration (user pushing up). The effect of friction, which pushes against the direction of motion, is small but visible. It is noted that, with the setup used, the free fall of the person occurs around $\psi = 0^o$ and the upwards acceleration of the chair occurs around $\psi = 25^o$. A large value of ψ produces an increase of the effective inertia (see eq. (22)). Therefore, it is advantageous to keep ψ small to minimize this effect. For instance, in a future implementation, the balancing lever will be designed such that it is horizontal when the person is standing. Simulations with and without taking into account B_3 were performed, and the results were always very close for the present setup. Therefore, the effect of the velocity — which rarely exceeded $1m/s$ in the experiments — on the effective inertia seems to be very small.

VI. Other Applications

The concept presented in this paper can also be used in other applications such as the development of training facilities for astronauts (see [15] for instance). By properly adjusting the balancing ratio, the device can emulate the gravity field of other planets or the moon and the trainees can walk in a large workspace without being hindered by floor-mounted mechanisms. Also, the device does not require the use of springs, which raise safety and reliability issues. This application is clearly illustrated in the accompanying video, where the effect of gravity compensation is demonstrated using leaping motions that are characteristic of astronauts evolving in a low-gravity environment.

VII. Conclusion

This paper presented a walking rehabilitation device that allows a person to walk freely on a floor over a large workspace. The basic principle of the device consists of a cable-routing system that follows the user in order to provide gravity compensation without hindering walking motions. The device naturally leads itself to a passive mechanism but can also be implemented as an active robotic system. Using a dynamic model, it was shown that a real implementation can be developed based on realistic requirements. Also, it was shown that the balancing principle based on the use of a counterweight can be exploited to minimize the spurious inertia. Finally, the experimental validation on a full-scale prototype provided design hints. Although there were some limitations on the experimental implementation, the prototype and the accompanying video clearly demonstrate the potential of the concept in a context of rehabilitation.

References

[1] M. Bouri, Y. Stauffer, C. Schmit, Y. Allemand, S. Gnemmi, R. Clavel, P. Metrailler and R. Brodard, 'The WalkTrainer: A Robotic System for Walking Rehabilitation' in IEEE Int. Conference on Robotics and Biomimetics, pp. 1616–1621, 2006.

[2] S. Jezernik, G.Colombo, T. Keller, H. Frueh and M. Morani, 'Robotic orthosis Lokomat: a rehabilitation and research tool', Neuromodulation: Technology at the Neural Interface, Vol. 6, No. 2, pp. 108–115, 2003.

[3] J. Jang, S. Yu, J. Han and C. Han, 'Development of a walking assistive service robot for rehabilitation of elderly people', in Service Robot Applications (Takahashi, ed.), In-Tech, August 2008.

[4] N. Siddiqi, F. Gazzani, J. Des Jardins and E.Y.S. Chao, 'The use of a robotic device for gait training and rehabilitation' Medicine Meets Virtual Reality, K.S. Morgan et al. (Eds.), IOS Press, 1997.

[5] C.Y. Lee and J.J. Lee, 'Walking-support robot system for walking rehabilitation: design and control', Artificial Life and Robotics, Vol. 4, No. 4, pp. 206–211, 2000.

[6] J. Patton, D.A. Brown, M. Peshkin, J.J. Santos-Munne, A. Makhlin, E. Lewis, E.J. Colgate and D. Schwandt, 'Design and Development of a Robotic Overground Gait and Balance Therapy Device', Topics in Stroke Rehabilitation, Vol. 15, No. 2, pp. 131–139, 2008.

[7] H. Schmidt, D. Sorowka, S. Hesse and R. Bernhardt, 'Development of a robotic walking simulator for gait rehabilitation', Biomed tech, Vol. 48, No. 10, pp. 281–286, Berlin, 2003.

[8] S. Perreault and C. Gosselin, 'Cable-driven parallel mechanisms: application to a locomotion interface', *ASME Journal of Mechanical Design*, Vol. 130, Article 102301, 2008.

[9] J. Yoon and J. Ryu, 'A novel locomotion interface with two 6-DOF parallel manipulators that allows human walking on various virtual terrains', International Journal of Robotics Research, Vol. 25, No. 7, pp. 689–708, 2006.

[10] D. Surdilovic and R. Bernhardt, 'STRING-MAN-Wire robot for gait rehabilitation: further development and testing', European Symposium on Technical Aids for Rehabilitation, January 25–26, Technical University of Berlin, 2007.

[11] www.bioness.com (2011).

[12] www.neurogymtech.com/products/bungee_walker.php (2011).

[13] www.kineadesign.com/portfolio/kineassist (2011).

[14] T. Laliberté, C. Gosselin and D. Gao, 'Closed-loop actuation routings for Cartesian SCARA-type manipulators', Proceedings of the ASME IDETC/CIE Conferences, August 15–18, Montreal, Canada, 2010.

[15] O. Ma, Q. Lu, J. McAvoy and K. Ruble, 'Concept study of a passive reduced-gravity simulator for training astronauts', Proceedings of the ASME IDETC/CIE Conferences, August 15–18, Montreal, Canada, 2010.